Male hoverflies (*Eristalis tenax*) do not use heuristic rules based on retinal size and speed to initiate indoor pursuits of artificial targets

Malin Thyselius[1], Yuri Ogawa[2], Richard Leibbrandt[3], Trevor J. Wardill[4], Paloma T. Gonzalez-Bellido[4] and Karin Nordström[1,2]*

[1]Department of Medical Cell Biology, Uppsala University, 75123 Uppsala, Sweden; [2]Flinders Health and Medical Research Institute, Flinders University, GPO Box 2100, Adelaide SA 5001, Australia; [3]College of Science and Engineering, Flinders University, GPO Box 2100, Adelaide SA 5001, Australia; [4]Department of Ecology, Evolution and Behavior, University of Minnesota, Saint Paul, MN 55108, USA

**To whom correspondence should be addressed, Karin.nordstrom@flinders.edu.au*

ORCIDs:

Malin Thyselius: 0000-0003-1342-8404

Yuri Ogawa: 0000-0002-9708-7063

Richard Leibbrandt: 0000-0003-2442-0782

Trevor Wardill: 0000-0002-2049-113X

Paloma Gonzalez-Bellido: 0000-0003-2201-991X

Karin Nordström: 0000-0002-6020-6348

Keywords

Hoverfly, *Eristalis tenax*, motion vision, 3D reconstruction, high-speed pursuit, following, categorization, dronefly, matched filter

Abstract

The ability to visualize small moving objects is vital for the survival of many animals, as these could represent predators or prey. For example, predatory insects, including dragonflies, robber flies and killer flies, perform elegant, high-speed pursuit of both biological and artificial targets. Many non-predatory insects, including male hoverflies and blowflies, also pursue targets during territorial or courtship interactions. Such predatory and non-predatory pursuits are often guided by heuristic rules based on the target image's retinal size, retinal speed, or both. To date, most hoverfly pursuits were studied outdoors. To investigate naturalistic hoverfly (*Eristalis tenax*) pursuits under more controlled settings, we constructed an indoor arena that was large enough to encourage naturalistic behavior. We presented artificial beads of different sizes, moving at different speeds, and filmed the pursuits with two cameras, allowing subsequent 3D reconstruction. Using this technique, we show that male *E. tenax* hoverflies are unlikely to use strict heuristic rules based on retinal size or speed to initiate pursuit, at least in our indoor setting. We show that male *E. tenax* start pursuits of beads that are moving either above or below them. Furthermore, we show that target pursuit behavior can be broken down into two stages. In the first stage the hoverfly attempts to decrease the distance to the target by flying at high speed. During the second stage the hoverfly's forward speed is correlated with the speed of the bead, so that it remains close to the bead without catching it. This could be useful for gathering more information before physical interaction.

Introduction

The ability to visually detect small moving objects can be essential for survival, as these could represent predators or prey. Such visual identification of prey is common in vertebrates. For example, to plan their attack, zebrafish larvae determine the speed and direction of motion of potential prey (Patterson et al., 2013). The zebrafish larvae first detect potential prey movement in their lateral visual field, and then adjust their own orientation to place the image of the prey in the frontal visual field, where their vision provides highest resolution (Mearns et al., 2020). Such strategies may provide more detailed visual information, which can then support attack decisions.

Visually driven, high-performance predatory attacks are also displayed by insects, including robber flies (Wardill et al., 2017), dragonflies (Olberg et al., 2000), killer flies (Wardill et al., 2015) and praying mantises (Nityananda et al., 2018). Killer flies (Wardill et al., 2015), some robber flies (Fabian et al., 2018) and dragonflies (e.g. Olberg et al., 2005; Olberg et al., 2000), detect their prey from a perch before launching a high-speed pursuit to catch their prey in mid-air. Killer flies decide whether to attack based on the ratio between the retinal size of the target image and its retinal speed (Wardill et al., 2015). The dragonflies *Sympetrum vicinum* and *Libellula luctuosa* have a preference for target beads with a diameter of 0.5 – 8 mm, with a peak preference for targets around 2 mm (Olberg et al., 2005), which in libelulid dragonflies seems to arise from the use of heuristic cues about the target's retinal size and speed (Lin and Leonardo, 2017).

Non-predatory *Eristalis sp.* hoverfly males pursue both conspecifics and heterospecifics encountered within their territories (Wellington and Fitzpatrick, 1981), but also other small moving targets presented to them (Fitzpatrick, 1981). As opposed to pursuits in more widely studied dragonflies (Olberg et al., 2000), killer flies (Wardill et al., 2015) and robber flies (Wardill et al., 2017), *Eristalis sp.* hoverflies often start their pursuit from a hovering or flying stance (Collett and Land, 1975b; Fitzpatrick, 1981; Wellington and Fitzpatrick, 1981). It has been suggested that hoverflies also use heuristic rules to determine when to initiate pursuit (Collett and Land, 1978). Indeed, as the size and typical flight speed of a conspecific is known (Golding et al., 2001; Nationalnyckeln, 2009), the male hoverfly can predict the conspecific's retinal size and speed at suitable distances (Collett and Land, 1978). This is supported by the observation that hoverflies in the field pursue artificial targets with a similar size to conspecifics (Collett and Land, 1978; Fitzpatrick, 1981; Fitzpatrick and Wellington,

1983; Maier and Waldbauer, 1979; Wellington and Fitzpatrick, 1981), which is 8 – 16 mm for *Eristalis sp.* (Nationalnyckeln, 2009). Such field studies also showed that *Eristalis sp.* males pursue artificial targets moving at 5 – 12.5 m/s (Collett and Land, 1978). However, female *Eristalis sp.* often move much slower than this (Thyselius et al., 2018), indicating that heuristic rules based on retinal speed may not be used, at least in the field.

Interestingly, *Eristalis sp.* hoverflies also pursue objects that are much larger than conspecifics, such as leaves (Maier and Waldbauer, 1979), butterflies, hornets and bumblebees (Wellington and Fitzpatrick, 1981). Other fly species also pursue targets that do not appear to be ecologically relevant. Predatory killer flies, for example, pursue targets that are 3 – 5 times their own size (Solano-Rojas et al., 2017; Wardill et al., 2015) and non-predatory blowflies pursue targets that are up to 3 times larger than themselves, but only rarely (Boeddeker et al., 2003; Lyneborg et al., 1975). When blowflies pursue larger beads, they fly further away from the bead, consistent with heuristic rules based on the bead's retinal size. If hoverflies similarly adjust their flight behavior to the target's retinal size, is currently unknown.

To investigate the nuances of hoverfly target responses with high resolution and behavioral control, we developed an indoor arena to record flight behavior in the lab. By making it large enough to encourage naturalistic behavior, we could reconstruct pursuits of beads of different sizes (6 mm to 38.5 mm diameter). We found that *E. tenax* males pursued these artificial targets in the arena, moving at speeds up to 2 m/s, starting their pursuit from a flying stance below as well as from above the bead. We found that pursuits were initiated across a large range of retinal sizes and speeds, arguing against the use of strict heuristic rules. We show that the hoverflies first accelerate to quickly get close to the artificial target, and then follow the target at a closer distance for up to several seconds. When the hoverfly is following the target at closer proximity, its translational speed is correlated with the bead speed, but not with its retinal size or speed, again arguing against the use of heuristic rules. Furthermore, we found that flight behavior was different when pursuing the 38.5 mm diameter bead, compared to the beads that were more similar to conspecific sizes. Indeed, compared to the 8 and 10 mm diameter beads, the hoverflies initiated pursuit of the 38.5 mm bead when it moved slower, they spent longer time distal to it, and they physically interacted with it more often.

Materials and methods

Animals

Eristalis tenax (Syrphidae) hoverflies were reared from farm collected larvae as described previously (Nicholas et al., 2018b). At any one time, we kept ten male and eight female *E. tenax* hoverflies in the flight arena (see below). We focused on male pursuit behavior, with the females present to encourage male competition. Males showed an interest in females about two weeks after emerging from the pupae and started pursuing artificial targets about two months after emerging.

Hoverflies had constant access to fresh pollen-sugar mix and water. All hoverflies lived in the arena until death, or until the time when their physical activity declined noticeably, when they were replaced, to keep the total number constant. Replacement hoverflies came from aged matched, or slightly younger, artificial hibernation stock (Nicholas et al., 2018b). In addition, all hoverflies were changed simultaneously four times, giving a total of five cohorts (Table 1). A total of 94 males and 80 female hoverflies were used in the study.

Flight arena and videography

A Plexiglass arena (1 m^3, Fig. 1A) was used for all experiments (custom designed by Akriform Plast AB, Sollentuna, Sweden). The arena was lit from above by two daylight fluorescent lamps (58 W/865, Nova Group AB, Helsingborg, Sweden) and two office fluorescent lamps, giving an average illuminance of 900 – 1200 lux (Amprobe LM-120 Light Meter, Amprobe, Everet, WA, USA). The hoverflies were kept on a 12:12 light:dark cycle at room temperature (19 – 20°C).

A fishing line (0.3 mm diameter) was looped around the arena, entering through two holes 0.7 m above the arena floor to form a horizontal path (Fig. 1A), since male eristaline hoverflies prefer horizontal target motion (Collett and Land, 1978). As a target we used a bead tied around the fishing line using a thinner fishing line (0.06 mm diameter). A stepper motor (23HS-108 MK.2 Stepper motor, Promoco Scandinavia AB, Täby, Sweden) together with a stepper driver (ST5-Q-NN DC input stepper driver, Promoco Scandinavia AB, Täby, Sweden) and a laptop were used to control the bead movement (similar to Wardill et al.,

2017). Ten programs with seven speeds each (up to 2 m/s) presented in a randomized order were used. Which program was used on any given day was randomized using a 10-sided die.

The bead started its motion 10 cm from one side of the arena (furthest away from the computer-motor setup, Fig. 1A), travelled 0.8 m to the other side, paused for 0.5 s, travelled back to its starting point, paused for 0.5, and then did the motion all over again, but at a different speed (see Sup Movie 1-6 for examples). The program was run continuously, pausing 3 seconds before looping.

Four bead sizes (6 mm, 8 mm, 10 mm and 38.5 mm in diameter) were used. The beads were painted glossy black using acrylic paint. The three smaller beads were made of glass (Panduro Hobby AB, Malmö, Sweden) and the 38.5 mm diameter bead of polystyrene (Clas Ohlson, Insjön, Sweden). The 6 mm and 10 mm diameter beads were used for 9 consecutive days each. The 38.5 mm bead was used in two periods of 7 and 2 consecutive days, respectively. The 8 mm bead was used for 10 consecutive days, and in addition as a control before and after the 6 mm bead experiments, and between the two periods of using the 38.5 mm bead.

We filmed for 39 min ± 2 min (mean ± SEM) per day using two cameras (120 frames/s, 640×480 pixels; EXFH25, Casio, Tokyo, Japan). Filming was done continuously, only pausing briefly every 10 minutes to start a new movie, since this was the maximum film length the cameras could save. The cameras were synchronized and calibrated as described previously (Thyselius et al., 2018; Wardill et al., 2017). Slight modifications to previous methods were made, so that only the synchronization flash was used, only the largest calibration checkerboard pattern (35 mm squares) was used, and the checkerboard pattern was printed on a polyester sheet (NeverTear, Arkitektkopia AB, Stockholm, Sweden) and glued to a board (done by Arkitektkopia AB, Stockholm, Sweden), to increase durability and stability.

Pursuit and cruising flights

We first identified cruising flights as those where a hoverfly was flying around but clearly not interacting with the bead, another hoverfly, or the arena walls (similar to Collett and Land, 1975a, see Sup Movie 7 for example). We arbitrarily selected ten cruising flights from male hoverflies, and ten from females, each 0.83 s (100 frames) long. We next manually identified video recordings where a male hoverfly clearly flew towards the bead and labelled these as visually identified pursuits (Table 2, see Sup Movie 1-6 for examples).

We tracked the 2D position of the hoverfly and the bead centroids using custom written Matlab scripts (Thyselius et al., 2018; Wardill et al., 2017), modified to facilitate the visual control and manual correction of the automatic tracking. We first established the 2D position of the hoverfly and the bead in each frame for each camera (as in Thyselius et al., 2018). Due to spatial resolution constraints only one point on the hoverfly and bead were tracked. We performed 2D reconstructions (Table 2) of all visually identified pursuits where neither the hoverfly nor the bead was obscured by arena features or another hoverfly. Pursuits where several hoverflies were interacting with each other and/or the bead were excluded.

The 2D data was smoothed using Matlab's lowess smoothing, which is a locally weighted linear regression method. We used a span of 2% of the total number of data points for smoothing the data. We then translated the 2D reconstructions to 3D (Table 2, Fig. 2A, B), using calibration files obtained from filming the checkerboard, synchronized with both cameras, and previously described methods (Thyselius et al., 2018; Wardill et al., 2017). Eight pursuits were excluded due to calibration issues, and five because the start of the trajectory was not recorded, the hoverfly hit the arena wall, or several hoverflies were flying.

Data quantification

In all equations below the x- and y-axes define the two sides, and the z-axis the height of the 3D reconstructions (Fig. 1A, 2A, B). *F* is used to describe the 3D coordinates of the hoverfly and *B* the 3D coordinates of the bead. The *frame rate* is 120 frames/s, and *t* subsequently defines time at 120 Hz resolution.

As in previous accounts (Collett and Land, 1975b; Varennes et al., 2019), we identified pursuit start based on a sharp turn followed by an increase in translational speed. For this purpose, we first quantified the hoverfly translational speed (F_s) from each pursuit, which was calculated using the Euclidian distance formula, using two consecutive frames of the hoverfly's 3D coordinates:

(Eq. 1) $$\mathrm{F_s}(t) = \sqrt{(F_x(t+1) - F_x(t))^2 + (F_y(t+1) - F_y(t))^2 + (F_z(t+1) - F_z(t))^2} / \left(\frac{1}{frame\ rate}\right)$$

We used the hoverfly translational speed (Fig. 2C) to quantify the speed ratio over 15 frames (125 ms, Fig. 2D):

(Eq. 2) $Speed\ ratio(t) = \frac{F_s(t+15)}{F_s(t)}$

We identified the largest speed ratio peak in the first third of the reconstructed pursuit (grey shading, Fig. 2D). When the bead speed was 0 or the reconstructed pursuit was longer than 500 frames (4.2 s), we identified the largest speed ratio peak within the first 180 frames (1.5 s).

To determine the hoverfly angular speed, we first calculated the hoverfly's flight heading based on its location change:

(Eq. 3) $\overrightarrow{Fh}(t) = (F_x(t+1) - F_x(t), F_y(t+1) - F_y(t), F_z(t+1) - F_z(t))$

We used the change in heading to quantify the hoverfly's angular speed:

(Eq. 4) Angular speed$(t) = arccos\ (\frac{\overrightarrow{Fh(t)} \cdot \overrightarrow{Fh(t+1)}}{\left|\overrightarrow{Fh(t)}\right| \cdot \left|\overrightarrow{Fh(t+1)}\right|})\ /(\frac{1}{frame\ rate})$

From this, we identified the largest angular speed peak in the 10 frames (83 ms) immediately preceding the largest speed ratio peak identified above (Eq. 2, grey shading, Fig. 2E). The time of the angular speed peak was used as pursuit start (i.e. *t = 0*) in all subsequent analyses.

To calculate the hoverfly acceleration, we first smoothed the hoverfly speed (*Fs*) using a moving average with a span of 10% of the data points. From the smoothed hoverfly speed we calculated acceleration as follows:

(Eq. 5) Acceleration$(t) = F_{s_smoothed}(t+1) - F_{s_smoothed}(t)$

3D distance (*d*) between the hoverfly and the bead was calculated using the formula for Euclidian distance and the 3D coordinates for the hoverfly (*F*) and bead (*B*):

(Eq. 6) $d(t) = \sqrt{(F_x(t) - B_x(t))^2 + (F_y(t) - B_y(t))^2 + (F_z(t) - B_z(t))^2}$

The retinal size of the bead's image (θ), as projected onto the hoverfly's eye, was calculated as follows:

(Eq. 7) $\theta(t) = 2 * arctan\ (\frac{\frac{w}{2}}{d(t)})$

Where w was the bead's physical diameter (8 mm, 10 mm or 38.5 mm) and $d(t)$, the distance between the bead and hoverfly, as given in Eq. 6.

We quantified the bead speed (B_s) using the bead's (B) 3D position:

(Eq. 8) $\mathrm{B_s}(t) = \sqrt{(B_x(t+1) - B_x(t))^2 + (B_y(t+1) - B_y(t))^2 + (B_z(t+1) - B_z(t))^2} / (\frac{1}{frame\ rate})$

The retinal speed of the bead (φ) projected onto the hoverfly's eye, was calculated using the law of cosine:

(Eq. 9) $\varphi(t) = arccos\ (\frac{d(t)^2 + d(t+1)^2 - \Delta d_B}{2d(t)d(t+1)}) / (\frac{1}{frame\ rate})$

Where Δd_B was the distance the bead travelled relative to the hoverfly's position from time t to time $t+1$. This data was smoothed using a span of 10% of the total number of data points.

We used the distance between the hoverfly and the bead to separate each pursuit into 'Distal' and 'Proximal'. For this, we first determined the distribution of all instantaneous distances from pursuit start, of all bead pursuits, for each bead size. We used the lower quartile as a cut-off to determine the proximal part of the pursuit, i.e. 13.7 cm for the 8 mm bead, 11.9 cm for the 10 mm bead and 8.9 cm for the 38.5 mm bead (Fig. 5D). Distal was defined as the time between pursuit start and the time when the hoverfly was last outside this cut-off, for pursuits where the hoverfly was further away than the cut-off at pursuit start. If the hoverfly was never within the cut-off distance, the minimum distance was used to determine the end of the distal stage. Proximal was identified as the time from when the hoverfly was first within the cut-off distance, allowing deviations further away if the hoverfly returned to within the cut-off distance within 200 ms.

When calculating the minimum distance between the bead and the hoverfly (Fig. 6), we measured the distance between the hoverfly centroid and the surface of the bead, by subtracting the bead radius from $d_{minimum}$ (Eq. 6).

We defined error angles separately in the azimuth and elevation plane. Each error angle (ε) was defined as the 2D angle between the hoverfly heading (*Fh*, Eq. 10a, b) and the line of

sight (*LoS*, Eq. 11a, b). The hoverfly heading vector (*Fh*, Eq. 10a, b) was calculated by subtracting the 2D position of the hoverfly between two consecutive frames, using:

(Eq. 10a) $\overrightarrow{Fh}(t)_{azimuth} = (F_x(t+1) - F_x(t), F_y(t+1) - F_y(t))$

(Eq. 10b) $\overrightarrow{Fh}(t)_{elevation} = (F_y(t+1) - F_y(t), F_z(t+1) - F_z(t))$

The line of sight (*LoS*, Eq. 11a, b) vector was defined as the bead's position relative to the hoverfly's position in the 2D plane:

(Eq. 11a) $\overrightarrow{LoS}(t)_{azimuth} = (F_x(t) - B_x(t), F_y(t) - B_y(t))$

(Eq. 11b) $\overrightarrow{LoS}(t)_{elevation} = (F_y(t) - B_y(t), F_z(t) - B_z(t))$

The resulting error angle (ε) was smoothed using a span of 4% of the total number of data points.

Visualization and statistics

Data analysis, statistics and plotting were done using Prism 9 (GraphPad Software Inc., San Diego, CA, USA) and Matlab (R2019b, The MathWorks, Inc., Natick, MA, USA). All data are shown as either individual data points or median +/- interquartile range, unless otherwise specified. We used a restricted maximum likelihood model to fit mixed-effects models to time aligned data. When quantifying values around the start of the pursuit, we calculated the mean from t_{-2} to t_{+2}, where t = pursuit start. Since most data were not normally distributed, we used Kruskal-Wallis tests followed by Dunn's multiple comparisons tests, or a Mann-Whitney tests, as appropriate. For circular data we used Matlab's Circular statistics toolbox (Berens, 2009).

To determine correlations, we analyzed the first 1 s of the time aligned data for all bead sizes to determine the correlation coefficient for time shifts of up to +/- 0.5 s (Fig. S3A, B) using Matlab's *corrcoef* function. From this data we extracted the time of the peak correlation. For visualization we then extracted the instantaneous data for each bead size individually, using the delay of peak correlation (Fig. 5G, H). In these plots we show the result of simple linear regression, citing the R^2 value or Prism's Spearman correlation as a goodness of fit measure.

Results

Male hoverflies pursue artificial targets in an indoor arena

To assert that *E. tenax* hoverflies behaved naturalistically in our indoor arena (Fig. 1A), we analyzed flights where the hoverflies did not interact with each other or the bead (see Methods), termed cruising flights. We calculated the instantaneous flight speed over 100 frames (0.83 s) for ten male and ten female cruising flights (see Sup Movie 7, for example). We found that the top cruising speed was just over 2 m/s with a median of 0.37 m/s for males and 0.35 m/s for females (Fig. 1B). This is similar to median flight speeds measured in the field (0.32 m/s, Golding et al., 2001; 0.34 m/s, Thyselius et al., 2018), suggesting that our arena enabled naturalistic flight speeds.

By filming with two cameras (Fig. 1A), we could reconstruct hoverfly pursuits of artificial targets in 3D. Two example 3D reconstructions show the location of the 8 mm diameter bead (diamonds) and the male hoverfly (circles) every 75 ms (Fig. 2A, B, Sup Movie 3, 4). Since hoverflies initiate pursuit while already on the wing (Collett and Land, 1975b), rather than from a perch, we defined pursuit start using a large increase in angular speed, followed by an increase in translational speed (Fig. 2C-E, and see Collett and Land, 1975b; Varennes et al., 2019). We found that the translational speed was faster when pursuing the smaller beads (Fig. 2F), but there was no difference in angular speed between the bead sizes (Fig. 2G). The hoverfly acceleration also increased after pursuit start (Fig. S1), but was much lower than the 33 m/s^2 previously measured from *Eristalis sp* in the field (Collett and Land, 1978).

Target image at pursuit start

To investigate if male hoverflies use heuristic rules when initiating pursuit of artificial targets in our indoor arena we quantified the target's physical speed, as well as its retinal speed and size at pursuit start. We first looked at what sizes the hoverflies pursued, and found that they pursued the black beads of all four sizes (6 mm, 8 mm, 10 mm and 38.5 mm in diameter, Sup Movie 1-6, Table 2). However, the 6 mm diameter bead was only rarely pursued (Table 2) and was therefore excluded from further quantification.

We found that male hoverflies started pursuit at a range of distances (from 5.6 cm to 91 cm, Fig. 3A), suggesting that the hoverflies could start pursuit from almost anywhere in the arena.

The median distance at pursuit start was 43 cm for the 8 mm bead, 48 cm for the 10 mm bead, and 44 cm for the 38.5 mm bead (Fig. 3A), but this was not significantly different. The coefficient of variation was 46% for the 8 mm bead, 41% for both the 10 and 38.5 mm beads (Fig. 3A). We next looked at the retinal size of the target at pursuit start and found that the larger bead had a significantly larger retinal size (green data, Fig. 3B), as expected from its larger physical size. The retinal size of the bead at pursuit start covered a broad range of 0.5 – 22°, with median sizes of 1.1°, 1.2° and 5.0°, respectively (Fig. 3B). The retinal size coefficients of variation were large, 91%, 66% and 79%, respectively (Fig. 3B).

The bead speed at pursuit start ranged from stationary to 2.0 m/s, with coefficients of variation of 73%, 86% and 138%, respectively (Fig. 3C). The median bead speeds at pursuit start were 0.8 m/s, 0.4 m/s and 0.2 m/s, but this trend was not significant ($p = 0.1$). The retinal speed of the target image at pursuit start was significantly lower for the largest bead size (Fig. 3D), with median speeds of 94°/s, 79°/s and 36°/s, respectively (Fig. 3D). This is similar to the retinal speed of other insects as viewed by feeding female *E. tenax* hoverflies (Thyselius et al., 2018). However, we found that the retinal speed coefficients of variation were large, 153%, 97% and 73%, respectively (Fig. 3D).

Taken together, due to the large coefficients of variation, it is unlikely that male *E. tenax* hoverflies use heuristic rules based on the target's retinal size or speed (Fig. 3B, D) to determine when to initiate pursuit. Killer flies use the ratio between the retinal size and speed to determine which targets to pursue (Wardill et al., 2015). However, we found that the coefficient of variation for this ratio was also large, 136%, 146% and 72%, respectively (not shown), making it unlikely that hoverflies use a similar rule. Neither did the hoverflies seem to selectively pursue targets from a narrow range of distances, physical sizes, nor bead speeds (Fig. 3A, C).

Flight behavior at start

The data above (Fig. 3) do not support the hypothesis that male *E. tenax* hoverflies use heuristic rules based on retinal size or speed to decide when to initiate pursuit. However, they could be using visual information from the bead to adjust its flight behavior at start. Hoverflies start their pursuit with a sharp turn followed by a translational speed increase (Collett and Land, 1975b; Varennes et al., 2019), here quantified as a speed ratio peak (Fig. 2E). We found that this peak speed ratio did not depend on the bead's physical diameter (Fig.

S2A), nor its retinal size (Fig. S2B). Neither did the speed ratio depend on the bead's translational speed (Fig. S2C), nor the retinal speed of the target image (Fig. S2D).

We next looked at whether the increased angular speed (Fig. 2E, G) associated with a sharp turn at pursuit start, depended on bead information, but found that it did not depend on the bead size (Fig. S2E), its retinal size (Fig. S2F), its translational speed (Fig. S2G), nor retinal speed (Fig. S2H). This is in contrast to work in the field, where the hoverfly's angular speed at pursuit start is correlated with the bead's retinal speed, which has been interpreted as an effort to put the target in the frontal visual field (Collett and Land, 1978). We found that the hoverflies' angular speed at pursuit start ranged from 460 to 13,000°/s, with median speeds of 2,960°/s for the 8 mm bead, 4,530°/s for the 10 mm bead and 4,230°/s for the 38.5 mm bead (Fig. S2E). This is similar to the turning speeds of male *Eristalis* pursuing targets in the field (Collett and Land, 1978).

We quantified the delay between the hoverfly's peak angular speed (blue dot, Fig. 2E) and the peak speed ratio (arrow, Fig. 2D) and found that this did not depend on the physical size of the bead (Fig. S2I) nor its retinal size (Fig. S2J). Neither did the delay depend on the bead's translational speed (Fig. S2K), nor its retinal speed (Fig. S2L). The median delay was 25 ms for the 8 mm bead, 17 ms for the 10 mm bead and 21 ms for the 38.5 mm diameter bead (Fig. 2I), similar to delays measured in the field (Collett and Land, 1975b). In summary, even if showing similar start behavior in our arena and in the field, with a sharp turn followed by a translational speed increase about 20 ms later, suggesting that the hoverflies behaved naturalistically, the hoverflies did not seem to use heuristic rules to control this behavior.

Flight pursuits starting from above or below

Killer flies pursue artificial beads from above as well as below (Rossoni et al., 2021). We found that male hoverflies also initiated pursuits of beads from a position above (black data, Fig. 4A) as well as below the bead (white data, Fig. 4A), with no difference between bead sizes. We next looked at the flight behavior at start (as in Fig. 2C-G, Fig. S2) and found that neither the speed ratio (Fig. 4B), nor the angular speed at start (Fig. 4C), depended on whether the pursuit started with the hoverfly below (open symbols, Fig. 4B, C) or above (closed symbols, Fig. 4B, C) the 8 mm diameter bead. Neither did the delay between the angular and translational speed peaks (Fig. 4D) depend on whether the pursuit started from below or above the bead.

In contrast, we found that pursuits that started from below the bead were initiated when the bead was significantly further away than pursuits from above (Fig. 4E). This could be because there was more space available below the bead track in our arena (Fig. 1A). The retinal size of the target image depended significantly on whether the pursuit started from above or below (Fig. 4F), consistent with the distance findings (Fig. 4E). We also found that when the hoverflies started their pursuit from above the 8 mm bead, the bead moved significantly faster than when they started the pursuit from below the bead (Fig. 4G). This resulted in a significant difference in the target image's retinal speed (Fig. 4H).

Male hoverflies divide their pursuits of artificial targets into two stages

Above we showed that the hoverfly behavior at pursuit start does not depend on the bead's physical size or speed, nor its retinal size or speed (Fig. 3, Fig. S2). We next investigated the hoverfly's behavior during pursuit. As expected, the distance between the male hoverfly and the bead decreased with time (Fig. 5A). This resulted in the target's retinal size increasing (Fig. 5B). There was no significant effect of bead size on the distance (Fig. 5A), but the retinal size was significantly larger for the 38.5 mm diameter bead (Fig. 5B), as expected from its larger physical size. The retinal speed of the target image also increased after pursuit start, but there was no significant effect of bead size (Fig. 5C).

To investigate the behavior during pursuit further, we separated each pursuit into two parts based on the distance between the hoverfly and the bead. For this purpose, we fist extracted all instantaneous distances from pursuit start onwards, as a function of bead size (Fig. 5D). This analysis showed that a large proportion of the pursuits were performed closer to the bead (Fig. 5D), as seen in the time-aligned data (Fig. 5A). The bead-to-hoverfly distance range was 0.5 – 92 cm, and the median distances were comparatively close (25, 22 and 20 cm, respectively, Fig. 5D). We used the lower quartile for each bead size (13.7, 11.9 and 8.9 cm, respectively, Fig. 5D, E) to separate each pursuit into a 'distal' and a 'proximal' component (see Methods).

We first quantified the time the hoverfly spent distal to the bead, and found that the range was large, from 83 ms to 3.9 s, with median durations of 0.81 s, 0.95 s and 1.5 s, respectively, which was significant (Fig. 5F). The time the hoverfly was distal to the bead increased linearly with the distance to the bead at pursuit start (R^2 values of 0.17, 0.25 and 0.19,

respectively, Fig. 5G), but the correlation was not significant for the 38.5 mm diameter bead (green data, Fig. 5G).

We next quantified the time the hoverfly was proximal to the bead and found that this ranged from 8.3 ms to 2.9 s, with median times of 0.39 s, 0.35 s and 0.69 s, respectively, but this difference was not significant (Fig. 5H). We hypothesized that the distal stage was optimized to rapidly decrease the distance to the bead (Fig. 5A, D-G), while the proximal stage (Fig. 5D, E, H) was aimed at staying close to the bead. To investigate this, we quantified the hoverfly translational speed after pooling the data for the three bead sizes and found that the flight speed was comparatively higher during the distal stage (black data, Fig. 5I), and significantly lower during the proximal stage (brown data, Fig. 5I). Previous work in the field showed pursuit speeds of up to 10 m/s (Collett and Land, 1978), which is faster than what we recorded, suggesting that the hoverflies did not reach their peak speed in our arena.

To investigate if hoverflies use heuristic rules to control their translational speed during pursuit, we calculated the correlation coefficients between hoverfly translational speed and the distance to the bead, the retinal size of the target image, the bead speed, and the retinal speed of the target image, during the first second of the distal stage (Fig. S3A). We found the strongest correlation between the hoverfly's translational speed and the bead's speed (solid data, Fig. S3A), with a peak correlation at -233 ms (dotted vertical line, Fig. S3A). When plotting each instantaneous flight speed as a function of the bead speed 233 ms previously (Fig. 5J) it becomes clear that even if they are correlated, there is large variation, with R^2 values of 0.26 for the 8 mm bead (purple data), 0.15 for the 10 mm bead (blue data), and only 0.010 for the 38.5 mm bead (green data, Fig. 5J). In addition, 233 ms is slow for typical insect reactions (e.g. Collett and Land, 1978; Mischiati et al., 2015; Varennes et al., 2020), so its biological relevance needs to be taken with caution. Taken together, this suggests that during the distal stage the hoverfly was not using heuristic rules to control its translational speed, but rather aiming to accelerate to rapidly decrease the distance to the bead (Fig. 5A, E, G, I).

In contrast to the distal stage, during the proximal stage the flight speed was significantly lower (brown data, Fig. 5I). To investigate if the hoverfly uses heuristic rules to adjust its translational speed to stay close to the bead, we did similar cross correlations and found the strongest correlation between the hoverfly's translational speed and the bead's speed (solid data, Fig. S3B) at -150 ms (dotted vertical line, Fig. S3B). When visualizing this with instantaneous hoverfly and bead speed data, during the proximal stage the R^2 value was 0.35

for the 8 mm bead (purple data), 0.21 for the 10 mm bead (blue data) and 0.39 for the 38.5 mm bead (green data, Fig. 5K). This suggests that when proximal to the bead the hoverfly attempted to follow its speed (Fig. 5K), rather than flying as fast as possible to catch it.

If indeed the hoverflies attempted to follow the bead, rather than catch it, this should be reflected in the minimum distance between the bead and the hoverfly. Indeed, we found that pursuits of the 8 and 10 mm beads rarely ended with the hoverfly grabbing or landing on the bead (median minimum distances 5.8 and 6.5 cm, respectively, Fig. 6). In contrast, the median distance between the hoverfly and the 38.5 mm bead was 0.99 cm (green data, Fig. 6), suggesting that the hoverflies often landed on the largest bead. This is interesting considering that they initiated pursuit of the 38.5 mm bead when it moved slower (Fig. 3C), and they spent longer time distal to it (Fig. 5F, G), suggesting that the hoverflies might have categorized it differently to the more conspecific-sized targets.

Error angles during pursuit

Our data show that male *Eristalis* hoverflies pursue beads starting from a position above as well as below the bead (Fig. 4). To investigate the relative location of the bead in more detail we quantified the error angle in the azimuth (Fig. 7A) and elevation plane (Fig. 7B). The error angle was defined as the angle between the hoverfly's heading, or direction of flight (black arrows, Fig. 7A, B), and the line of sight, i.e. the straight line connecting the hoverfly and the bead (dashed lines, Fig. 7A, B; Gonzalez-Bellido et al., 2016; Land and Collett, 1974).

We found that 100 ms before pursuit start there was no preferential error angle, neither in the azimuth (Fig. 7C*i*) nor the elevation plane (Fig. 7D*i*). We next quantified the error angle at the start of the distal stage and found that there was no preferred azimuth error angle (Fig. 7C*ii*), nor in the elevation plane (Fig. 7D*ii*). Previous work suggested that the hoverfly's angular turn at pursuit start is correlated with the bead's error angle (Collett and Land, 1978). We found no such correlation between angular speed and the error angle for the two smaller bead sizes (blue and purple, Fig. S4), whereas there was a correlation for the 38.5 mm bead, with an R^2 value of 0.10 (green data, Fig. S4).

100 ms into the distal stage we found a dorso-anterior mean error angle, but the preference was small as other error angles were common (red, Fig. 7C*iii*, D*iii*). At the start of the proximal stage, the mean error angle was strongly anterior (red, Fig. 7C*iii*, D*iv*), but this

strong directional preference had decreased 100 ms into the proximal stage of the pursuit (red, Fig. 7C*v*, D*v*). Indeed, the error angles 100 ms into the proximal stage of the pursuit (red, Fig. 7C*v*, D*v*) were similar to the error angles 100 ms into the distal stage (red, Fig. 7C*iii*, D*iii*). Taken together, our data suggest the hoverflies attempted to keep the target image roughly anterior relative to its direction of flight, but there was a large variation (Fig. 7).

Discussion

We here showed that *E. tenax* males pursue artificial targets ranging from 6 mm to 38.5 mm in diameter (Table 2) in an indoor flight arena (Fig. 1A, 2, Sup Movie 1-6). We show that male *E. tenax* pursue targets from above as well as below (Fig. 4, 7), with pursuits lasting several seconds (Fig. 5). At the start of the pursuit the hoverflies fly fast to decrease the distance to the bead, whereas they match their translational speed to the bead when they are proximal (Fig. 5, S3), without actually catching it (Fig. 6). We show that male *E. tenax* are unlikely to use heuristic rules based on retinal size or speed to initiate pursuit of artificial targets (Fig. 3, Fig. S2), and that pursuits of the largest bead (green data, Fig. 3D, 5F, 6) differed from pursuits of the smaller beads.

Naturalistic behavior in an artificial arena

Dragonflies (Mischiati et al., 2015), blowflies (Boeddeker et al., 2003; Varennes et al., 2019) and killer flies (Wardill et al., 2015) pursue artificial targets indoors. However, even if hoverflies have previously been shown to fly in indoor arenas (Chen et al., 2013; Geurten et al., 2010), they have not performed pursuit behavior, which could be because of the sizes of these arenas. Indeed, male hoverfly pursuits are likely used to increase their mating success (Fitzpatrick, 1981; Maier and Waldbauer, 1979) and *Eristalis* males keep 0.22 – 2 m^3 large territories around flowers where females feed (Fitzpatrick, 1981; Fitzpatrick and Wellington, 1983; Wellington and Fitzpatrick, 1981). The territorial size variation is partially dependent on the environment, with territories often following the size of the flower patch it is kept around, but territories as small as 0.22 – 0.36 m^3 may be sufficient for an *Eristalis sp.* male (Wellington and Fitzpatrick, 1981), even if the pursuits themselves often stretch over larger distances (Collett and Land, 1978). We made our arena large enough (Fig. 1A) to encompass a more typical territory (Fitzpatrick, 1981; Fitzpatrick and Wellington, 1983; Wellington and Fitzpatrick, 1981), and the hoverflies did indeed pursue artificial targets in this (Table 2, Sup

Movie 1-6). However, the large size of the arena limited our reconstructions to 1-point tracking (Fig. 2A, B).

We found that the pursuits lasted for several seconds (Fig. 5F, H). Previous work showed *Eristalis sp.* pursuits ranging from 0.2 to 0.5 s (Collett and Land, 1978), *V. pellucens* pursuits ranging from 0.3 to 0.9 s (Collett and Land, 1978) and *S. pipiens* pursuits ranging from 0.8 to 3.6 s (Collett and Land, 1975a). However, quantification of pursuit length was not an explicit aim in any of those studies, so direct comparisons of pursuit lengths in the field and in our indoor arena are difficult. We found that the pursuit flight speed (Fig. 2F, 5I) was lower than the 10 m/s that has been recorded in the field (Collett and Land, 1978). In addition, the acceleration (Fig. S1) was much lower than the 33 m/s^2 measured in the field (Collett and Land, 1978). Therefore, while the hoverflies performed target pursuits in the arena, they were not flying as fast as they may do in the field. However, the high angular speeds associated with pursuit start (Fig. 2E, G, S2E) were similar to those measured in the field (Collett and Land, 1978), suggesting that turning behaviors were naturalistic.

Heuristic rules to determine pursuit start

It has been suggested that hoverflies use matched filters, also referred to as heuristic rules, to initiate conspecific pursuit (Collett and Land, 1978). However, we found that male *E. tenax* initiated pursuit of beads where the retinal size and speed covered a large range of values (Fig. 3B, D), arguing against this. We defined pursuit start as a saccade like turn followed by a translational speed increase (Fig. 2C-G, Sup Movie 1-6), consistent with previous work (see e.g. Collett and Land, 1975b; Varennes et al., 2019). The hoverflies did not appear to adapt this behavior to the retinal size or speed of the target (Fig. S2), as previously suggested (Collett and Land, 1978). From our data it is thus unclear what cues trigger the hoverfly to start pursuit. Since all our experiments used a black bead moving against a brighter background (Fig. 1A, Sup Movie 1-6), it would in future work be interesting to determine if the dark contrast of the bead against a brightly lit background is an important driver. Indeed, the target tuned neurons in the hoverfly visual system that are believed to underlie pursuit behaviors respond strongly to dark contrast targets subtending 1-3° (Barnett et al., 2007; Nicholas et al., 2018a), with a size tuning curve similar to the size of the retinal image at pursuit start (Fig. 3B).

Hoverfly males have been suggested to pursue targets their own size (Collett and Land, 1978). In the field *Eristalis sp.* hoverflies pursue peas with a diameter of 7 mm, while the slightly larger *V. pellucens* pursue cylindrical wooden blocks with a diameter and height of 15 mm (Collett and Land, 1978). We found that *E. tenax* males did indeed pursue targets their own size (8 mm and 10 mm diameter beads, Sup Movie 2-5). In addition, they pursued slightly smaller beads (6 mm diameter, Sup Movie 1), but only rarely (Table 2). The males did, however, also pursue the largest bead (38.5 mm diameter, Sup Movie 6), which is 2 - 3 times the length of *E. tenax* (14 mm - 16 mm, Nationalnyckeln, 2009). This supports field observations that *Eristalis sp.* males may pursue leaves (Maier and Waldbauer, 1979), butterflies, hornets and bumblebees (Wellington and Fitzpatrick, 1981). Interestingly, however, when pursuing the largest bead, the hoverflies flew slower (green, Fig. 2F), pursued beads that moved slower (green, Fig. 3C), spent longer pursuing the beads (green, Fig. 5F), and often landed on them (green, Fig. 6). This suggests that the largest beads might have been categorized as a landing object, such as a flower or a post, rather than as another insect.

Previous work suggested that *E. tenax* males pursue targets traveling at female flight speeds (Collett and Land, 1978). However, these studies showed that males of the small *S. pipiens* hoverfly pursue targets moving at around 0.2 – 0.8 m/s (Collett and Land, 1975a), that large *V. pellucens* hoverflies may pursue targets moving at 5 m/s and 8 m/s, and the intermediate sized *Eristalis sp.* pursue targets moving at 5 – 12.5 m/s (Collett and Land, 1978), which is faster than typical female *Eristalis sp.* flight speeds (Thyselius et al., 2018). We here showed that hoverflies also pursue beads moving comparatively slowly, and even when stationary (Fig. 3C). This is important since male *E. tenax* often wait for females to land before trying to mate with them (Fitzpatrick, 1981). Importantly, male *E. tenax* are capable of flying much faster than what we recorded, up to 10 m/s (Collett and Land, 1978). Indeed, even in our experiments, which took place in a limited physical space, thus likely limiting the flight speed, we found instantaneous pursuit speeds of up to 3.3 m/s (Fig. 5J). Taken together, this could suggest that the males in our arena perceived the bead as a male competitor rather than a cruising female. Alternatively, when escaping from an incoming insect in the field female *E. tenax* fly at up to 1.5 m/s (Thyselius et al., 2018), so the bead might also be perceived as an escaping female. Indeed, the median retinal size at pursuit start (1.1° - 5.0°, Fig. 3B) was close to the retinal size (median 2.7 – 6.8°) of an incoming insect when a female hoverfly decides to leave her food flower (Thyselius et al., 2018). Thus, when male *E. tenax* pursue

artificial targets moving faster than female cruising speed (Fig. 3C, 5J, K; and see Collett and Land, 1978) they may perceive the bead as an escaping female.

Pursuit style

Differences in visual ecology abound between aerial insects, and this is reflected in their visual adaptations. For example, whereas the acuity in the killer fly eye appears rather homogenous, dragonfly and robber fly eyes often boast areas with improved spatial and temporal resolution, so called acute zones, which are equivalent to vertebrate foveas. Indeed, both dragonflies (Olberg et al., 2007) and robber flies (Wardill et al., 2017) attempt to keep the image of their target in this acute zone during pursuit, a strategy shared with non-predatory dipterans that also pursue moving objects flying by at high speed, such as houseflies (Wagner, 1986; Wehrhahn et al., 1982) and males of the hoverfly *Syritta pipiens* (Collett and Land, 1975a). We found that male *E. tenax* pursue targets from above as well as from below (Fig. 4, 7). The male *E. tenax* dorso-frontal bright zone provides high contrast sensitivity in a large part of the frontal visual field, but the largest facets are found in a small dorso-frontal zone, 30 – 40° above the equator (Straw et al., 2006). Even if we did not reconstruct the head movements during pursuits, the target image is unlikely to fall within the dorso-frontal bright zone when the hoverfly is flying above the bead (Fig. 4, 7D).

We broke down each pursuit into two stages, where the first distal stage appeared to be optimized to rapidly decrease the distance to the target, and the second proximal stage to staying close to the target (Fig. 5). For *E. tenax* males the goal may not be to catch a target (Fig. 6), but to either chase it out of its territory if it is an intruder, or to stay close until it lands if it is a potential mate. Indeed, staying close to the target allows the hoverfly to gather more information. *Eristalis sp.* males often chase intruders out of their territories without contact (Fitzpatrick, 1981). The males also often follow females, waiting for them to settle before mating, rather than grasping them in the air (Fitzpatrick, 1981). Indeed, we found that *E. tenax* males could follow the artificial target for many seconds (Fig. 5H). We showed that when proximal the hoverfly matched its own translational speed to the speed of the target (Fig. 5K), likely to stay in close vicinity, even if it was well within its capacity to speed up (see e.g. Fig. 5I) and catch the target. Indeed, they rarely got close enough to the 8 or 10 mm beads to suggest physical contact (Fig. 6).

When blowflies pursue beads they sometimes follow it for a long time, without catching it, during which they keep a fixed distance to the bead (Boeddeker et al., 2003). They do this by controlling their forward speed based on the retinal size of the target (Boeddeker et al., 2003), so that smaller beads (physical sizes) end up being followed at a closer distance, compared to larger beads. However, we did not see a correlation between hoverfly flight speed and the target's retinal size (dotted data, Fig. S3A, B), nor did we find a similar relationship between bead size and distance (Fig. 5A, D). In contrast to blowflies, *S. pipiens* hoverflies control their forward speed based on the distance to the target (Collett and Land, 1975a), as do houseflies (Wehrhahn et al., 1982). We found only a weak correlation between hoverfly flight speed and distance to the bead (dashed data, Fig. S3).

Thus, whereas blowflies keep the distance to the target relatively constant (Boeddeker et al., 2003), the hoverflies did not seem to do the same (Fig. 5, S3), suggesting that even if they follow the bead, they do not have as precise a control mechanism for this behavior. Furthermore, we found the strongest correlation between bead speed and hoverfly speed at a delay of 150 ms (Fig. S3B), which is slow in comparison to other insects. Houseflies, for example, have a 20 ms delay between changes in flight speed based on the distance to the target (Wehrhahn et al., 1982).

Nevertheless, it might be beneficial for hoverflies to keep a longer distance to the target to avoid physical and potentially lethal contact. Indeed, physical contact is often seen as a last resort in conflict across the animal kingdom: hornets click their jaws when threatened before using their stinger (Cobey et al., 2020), snakes wrestle without their fangs when fighting conspecifics (Smith and Price, 1973), and cichlids when presented with a mirror mimicking a conspecific choose non-physical displays as their most common response (Ros et al., 2006). Indeed, escalated attack is costly (Smith and Price, 1973), fighting animals also notice predators later and thus face an increased risk of getting eaten (Jakobsson et al., 1995). Could it thus be that *E. tenax* have developed a strategy that will take them close to but rarely in contact with their targets?

Acknowledgments

We thank Annika Olsén, Mats Thyselius, Moa Thyselius, AB Cederholms Lantbruk, Louise Gustafsson, current and past lab members for valuable feedback during the many stages of this work.

Funding

This research was funded by the US Air Force Office of Scientific Research (AFOSR, FA9550-19-1-0294 and FA9550-15-1-0188) and the Australian Research Council (ARC, FT180100289 and DP210100740).

Data availability

All data and analysis scripts will be deposited to DataDryad: [Link to be inserted here]

References

Barnett, P. D., Nordström, K. and O'Carroll, D. C. (2007). Retinotopic organization of small-field-target-detecting neurons in the insect visual system. *Curr Biol* **17**, 569-578.

Berens, P. (2009). CircStat: A MATLAB Toolbox for Circular Statistics. *Journal of Statistical Software* **31**, 21.

Boeddeker, N., Kern, R. and Egelhaaf, M. (2003). Chasing a dummy target: smooth pursuit and velocity control in male blowflies. *Proc Biol Sci* **270**, 393-9.

Chen, M. W., Zhang, Y. L. and Sun, M. (2013). Wing and body motion and aerodynamic and leg forces during take-off in droneflies. *Journal of the Royal Society Interface* **10**, 1-12.

Cobey, S., Jensen, M. and Lawrence, T. (2020). The Asian giant hornet: what the public and beekeepers need to know. *Washington State University Extension Publications*, 1-8.

Collett, T. S. and Land, M. F. (1975a). Visual control of flight behaviour in the hoverfly, *Syritta pipiens* L. *J Comp Physiol A* **99**, 1-66.

Collett, T. S. and Land, M. F. (1975b). Visual spatial memory in a hoverfly *J Comp Physiol* **100**, 59-84.

Collett, T. S. and Land, M. F. (1978). How hoverflies compute interception courses. *J Comp Physiol A* **125**, 191-204.

Fabian, S. T., Sumner, M. E., Wardill, T. J., Rossoni, S. and Gonzalez-Bellido, P. T. (2018). Interception by two predatory fly species is explained by a proportional navigation feedback controller. *Journal of The Royal Society Interface* **15**.

Fitzpatrick, S. M. (1981). Territorial aggression among males of three syrphid species. In *Plant Science*, vol. MSc: University of British Columbia.

Fitzpatrick, S. M. and Wellington, W. G. (1983). Contrasts in the territorial behavior of three species of hover flies (Diptera: Syrphidae). *Can Entomol* **115**, 559-566.

Geurten, B., Kern, R., Braun, E. and Egelhaaf, M. (2010). A syntax of Hoverfly Flight Prototypes. *Journal of Experimental Biology* **213**, 2461-2475.

Golding, Y. C., Ennos, A. R. and Edmunds, M. (2001). Similarity in flight behaviour between the honeybee *Apis mellifera* (Hymenoptera: apidae) and its presumed mimic, the dronefly *Eristalis tenax* (Diptera: syrphidae). *J Exp Biol* **204**, 139-45.

Gonzalez-Bellido, P. T., Fabian, S. T. and Nordström, K. (2016). Target detection in insects: optical, neural and behavioral optimizations. *Curr Opin Neurobiol* **41**, 122-128.

Jakobsson, S., Brick, O. and Kullberg, C. (1995). Escalated fighting behaviour incurs increased predation risk. *Animal Behaviour* **49**, 235-239.

Land, M. F. and Collett, T. S. (1974). Chasing behaviour of houseflies (*Fannia canicularis)*. *J Comp Physiol A* **89**, 331-357.

Lin, H. T. and Leonardo, A. (2017). Heuristic Rules Underlying Dragonfly Prey Selection and Interception. *Curr Biol* **27**, 1124-1137.

Lyneborg, L., Coulianos, C.-C. and Anthon, H. (1975). Vad jag finner på sandmark och hed. Stockholm: Almqvist & Wiksell.

Maier, C. T. and Waldbauer, G. P. (1979). Dual mate-seeking strategies in male syrphid flies (Diptera: Syphidae). *Ann Entomol Soc Am* **72**, 54-61.

Mearns, D. S., Donovan, J. C., Fernandes, A. M., Semmelhack, J. L. and Baier, H. (2020). Deconstructing hunting behavior reveals a tightly coupled stimulus-response loop. *Curr Biol* **30**, 54-69.e9.

Mischiati, M., Lin, H., Herold, P., Imler, E., Olberg, R. and Leonardo, A. (2015). Internal models direct dragonfly interception steering. *Nature* **517**, 333-338.

Nationalnyckeln. (2009). Nationalnyckeln till Sveriges flora och fauna. Tva□vingar: Blomflugor: Diptera: Syrphinae . *Artdatabanken, SLU*.

Nicholas, S., Supple, J., Leibbrandt, R., Gonzalez-Bellido, P. T. and Nordström, K. (2018a). Integration of small- and wide-field visual features in Target-Selective Descending Neurons of both predatory and non-predatory dipterans. *J Neurosci* **38**, 10725-10733.

Nicholas, S., Thyselius, M., Holden, M. and Nordström, K. (2018b). Rearing and long-term maintenance of *Eristalis tenax* hoverflies for research studies. *JoVE*, e57711.

Nityananda, V., Tarawneh, G., Henriksen, S., Umeton, D., Simmons, A. and Read, J. C. A. (2018). A Novel Form of Stereo Vision in the Praying Mantis. *Curr Biol* **28**, 588-593.e4.

Olberg, R. M., Seaman, R. C., Coats, M. I. and Henry, A. F. (2007). Eye movements and target fixation during dragonfly prey-interception flights. *J Comp Physiol A* **193**, 685-693.

Olberg, R. M., Worthington, A. H., Fox, J. L., Bessette, C. E. and Loosemore, M. P. (2005). Prey size selection and distance estimation in foraging adult dragonflies. *J Comp Physiol A* **191**, 791-7.

Olberg, R. M., Worthington, A. H. and Venator, K. R. (2000). Prey pursuit and interception in dragonflies. *J Comp Physiol A* **186**, 155-162.

Patterson, B. W., Abraham, A. O., MacIver, M. A. and McLean, D. L. (2013). Visually guided gradation of prey capture movements in larval zebrafish. *J Exp Biol* **216**, 3071-83.

Ros, A. F., Becker, K. and Oliveira, R. F. (2006). Aggressive behaviour and energy metabolism in a cichlid fish, *Oreochromis mossambicus*. *Physiology & Behavior* **89**, 164-170.

Rossoni, S., Fabian, S. T., Sutton, G. P. and Gonzalez-Bellido, P. T. (2021). Gravity and active acceleration limit the ability of killer flies (*Coenosia attenuate*) to steer towards prey when attacking from above. *Journal of the Royal Society Interface* **18**, 20210058.

Smith, J. M. and Price, G. R. (1973). The logic of animal conflict. *Nature* **246**, 15-18.

Solano-Rojas, Y., Pont, A., De Freitas, J., Moros, G. and Goyo, Y. (2017). First record of Coenosia attenuata Stein, 1903 (Diptera: Muscidae) in Venezuela.

Straw, A. D., Warrant, E. J. and O'Carroll, D. C. (2006). A 'bright zone' in male hoverfly (*Eristalis tenax*) eyes and associated faster motion detection and increased contrast sensitivity. *J Exp Biol* **209**, 4339-54.

Thyselius, M., Gonzalez-Bellido, P. T., Wardill, T. J. and Nordström, K. (2018). Visual approach computation in feeding hoverflies. *Journal of Experimental Biology* **221**, jeb177162.

Varennes, L., Krapp, H. G. and Viollet, S. (2020). Two pursuit strategies for a single sensorimotor control task in blowfly. *Sci Rep* **10**, 20762.

Varennes, L. P., Krapp, H. G. and Viollet, S. (2019). A novel setup for 3D chasing behavior analysis in free flying flies. *J Neurosci Methods* **321**, 28-38.

Wagner, H. (1986). Flight performance and visual control of flight of the free-flying housefly (*Musca domestica* .L.) II. Pursuit of targets. *Philosophical Transactions of the Royal Society of London. B, Biological Sciences* **312**, 553-579.

Wardill, T., Fabian, S., Pettigrew, A., Stavenga, D. G., Nordström, K. and Gonzalez-Bellido, P. (2017). A novel interception strategy in a miniature robber fly with extreme visual acuity. *Curr Biol* **27**, 854-859.

Wardill, T. J., Knowles, K., Barlow, L., Tapia, G., Nordström, K., Olberg, R. M. and Gonzalez-Bellido, P. T. (2015). The Killer Fly Hunger Games: Target Size and Speed Predict Decision to Pursuit. *Brain, Behav Evol* **86**, 28-37.

Wehrhahn, C., Poggio, T. and Bulthoff, H. (1982). Tracking and Chasing in Houseflies (*Musca*) - an Analysis of 3-D Flight Trajectories. *Biological Cybernetics* **45**, 123-130.

Wellington, W. and Fitzpatrick, S. (1981). Territoriality in the drone fly, *Eristalis tenax* (Diptera, Syrphidae). *Can Entomol* **113**, 695-704.

Figure legends

Figure 1. An indoor arena for hoverfly pursuits of artificial targets

A) We developed a flight arena consisting of a Plexiglas cube (1 m^3) with a fishing line that looped around outside to form a horizontal path 0.7 m above the arena floor. A bead was suspended from the fishing line with its movement controlled by a rotor (lower left), that was programmed by a laptop (left). For clarity, the hoverfly and bead are shown out of proportion and only one of the 18 hoverflies is shown. Experiments were filmed at 120 frames/s using two synchronized cameras (front). B) Instantaneous hoverfly flight speed during cruising measured across 100 consecutive frames (total of 0.83 s) for 10 male (black) and 10 female (grey) flights. Horizontal solid lines show the median and the dashed lines show the interquartile ranges.

Figure 2. Pursuit start definition

A) An example of a male *E. tenax* (circles) pursuing an 8 mm diameter bead (diamonds) programmed to move at 1.3 m/s. The data show the locations of the hoverfly and bead every 75 ms. B) An example of a male *E. tenax* (circles) pursuing an 8 mm diameter bead (diamonds) programmed to move at 1.6 m/s. In panels A and B the pursuits are color coded to indicate time. C) The hoverfly's translational speed of the example reconstruction in panel A as a function of time. D) The speed ratio of the speed shown in panel C (since the speed ratio is calculated across 15 frames, the ratio is 125 ms shorter than the speed). We identified the largest peak (arrow) in the first third of the pursuit (shaded area). E) The hoverfly's angular speed during the same trajectory. We identified the pursuit start as the largest and sharpest peak (blue circle) in the 83 ms immediately preceding the speed ratio peak (shaded area). F) The hoverflies' translational speed at pursuit start. The data show the median +/- interquartile range, color coded according to bead size. The star (*) indicates a significant difference between the 38.5 mm diameter bead and the two smaller beads ($p < 0.05$, mixed-effects model, followed by Tukey's multiple comparisons test). G) The hoverflies' angular speed at pursuit start. The data show the median +/- interquartile range. There was no significant effect of bead size.

Figure 3.* E. tenax *hoverflies do not use a matched filter to initiate pursuit

A) The distance between the hoverfly and the bead at pursuit start. B) The retinal size of the target image at pursuit start. C) The translational speed of the bead at pursuit start. D) The retinal speed of the target image. The data were analyzed using Kruskal-Wallis tests, with * indicating $p < 0.05$ and **** for $p < 0.0001$.

Figure 4.* E. tenax *hoverflies initiate pursuits from above as well as below the bead

A) The position of the hoverfly relative to the bead at pursuit start, as a function of bead size (N = 50, 26 and 12, respectively). There was no significant difference between the bead sizes ($p = 0.93$, chi square test). B) The speed ratio of the hoverfly following pursuit start, as a function of whether the hoverfly was below (open symbols) or above (closed symbols) the 8 mm bead at pursuit start. C) The hoverflies' angular speed at pursuit start, as a function of whether the hoverfly was below or above the bead. C) The delay between the hoverflies' angular and translational speed ratio peaks, as a function of whether the hoverfly was below or above the bead. E) The distance between the hoverfly and the bead, when the hoverfly was below or above the bead at pursuit start. F) The retinal size of the target image as seen by the hoverfly at pursuit start, when the hoverfly was below or above the bead. G) The bead speed at pursuit start, when the hoverfly was below or above the bead. H) The retinal speed of the target image as seen by the hoverfly at pursuit start, when the hoverfly was below or above the bead. Significance was investigated using Mann-Whitney tests with ** for $p < 0.01$.

Figure 5. The distal and proximal part of the pursuit

A) The distance between the hoverfly and the bead as a function of time, color coded according to bead size. B) The retinal size of the target image as seen by the pursuing male hoverfly. C) The retinal speed of the target image as seen by the pursuer. The data in panels A-C were analyzed using mixed-effect models, followed by Tukey's multiple comparisons test, with **** for $p < 0.0001$. D) All instantaneous distances between the hoverfly and the bead across all pursuits. Horizontal lines show the median (black) and interquartile ranges (colored). The shaded boxes delineate the lower quartile (brown shading) from the rest of the data (grey shading), which was used to define distal from proximal. E) The distance between the hoverfly and the bead for an example pursuit. The time between pursuit start and when first within the 8 mm bead's cut-off distance (13.7 cm, dashed line) was defined as distal

(grey shading). We defined the time within this cut-off distance as proximal ("Prox.", brown shading). F) The time the hoverfly was distal to the bead as function of bead size. The data were analyzed using a Kruskal-Wallis test ($p = 0.025$). G) The time the hoverfly was distal to the bead as function of the distance to the bead at pursuit start. The lines show the results of a linear regression ($R^2 = 0.17$, 0.25 and 0.19, respectively). H) The time the hoverfly was proximal to the bead as function of bead size. The data were analyzed using a Kruskal-Wallis test. I) The hoverfly speed as a function of time, color coded according to whether the speed came from the distal (black) or proximal part of the pursuit (brown). The data show the median +/- interquartile range, and the * indicates a significant difference after being analyzed using mixed-effect models, followed by Tukey's multiple comparisons test. J) The hoverflies' instantaneous translational speeds as a function of the bead speed 233 ms previously, during the distal part of the pursuit. The lines show linear regression ($R^2 = 0.26$, 0.15 and 0.009, respectively). K) The hoverflies' instantaneous translational speeds as a function of the bead speed 150 ms previously, from the proximal part of the pursuit. The lines show linear regression ($R^2 = 0.35$, 0.21 and 0.39, respectively).

Figure 6. The hoverflies land on the largest bead, but not the others

The minimum distance between the hoverfly and the bead, here defined as the distance between the surface of the bead and the center of the hoverfly. The minimum distance depended significantly on bead size ($p = 0.0013$, Kruskal-Wallis test).

Figure 7. The error angle

A) We defined the error angle (ε) as the angle between the hoverfly's heading (black arrows) and the direct line connecting the hoverfly's position and the bead's location (grey dashed line, often referred to as Line of Sight). The diagram shows this in the azimuth plane. B) The error angle in the elevation plane. C) The error angle in the azimuth plane across 5 different time points: *i)* 100 ms before pursuit start (N = 73), *ii)* when distal at pursuit start (N = 83, *iii)* 100 ms into the distal part of the pursuit (N = 82), *iv)* when first being proximal to the bead (N = 73), and *v)* 100 ms into the proximal part of the pursuit (N = 69). D) The elevation error angle across the same 5 time points. In panels C, D the black dots show the error angle for each individual pursuit of the 8, 10 and 38.5 mm diameters beads. The histograms show the distribution of error angles within 15° bins. The red line shows the resulting mean vector.

Table 1. Hoverfly cohorts used in the experiments and their age when placed in the flight arena

Cohort #	Age of hoverflies at start
1	0-1 days
2	5 months
3	2-3 months
4	3 weeks
5	4 days

Table 2. Number of pursuits at each stage of the analysis

Bead size (mm)	**6 mm**	**8 mm**	**10 mm**	**38.5 mm**
Recording time (h)	5.8	10.1	6.8	5.2
Visually identified (N)	6	81	39	41
Pursuit frequency (N/h)	1.0	8.0	5.7	7.9
2D reconstructions (N)	5	56	30	15
3D reconstructions (N)	5	50	26	12
Distal (N)		45	26	12
Proximal (N)		43	19	11

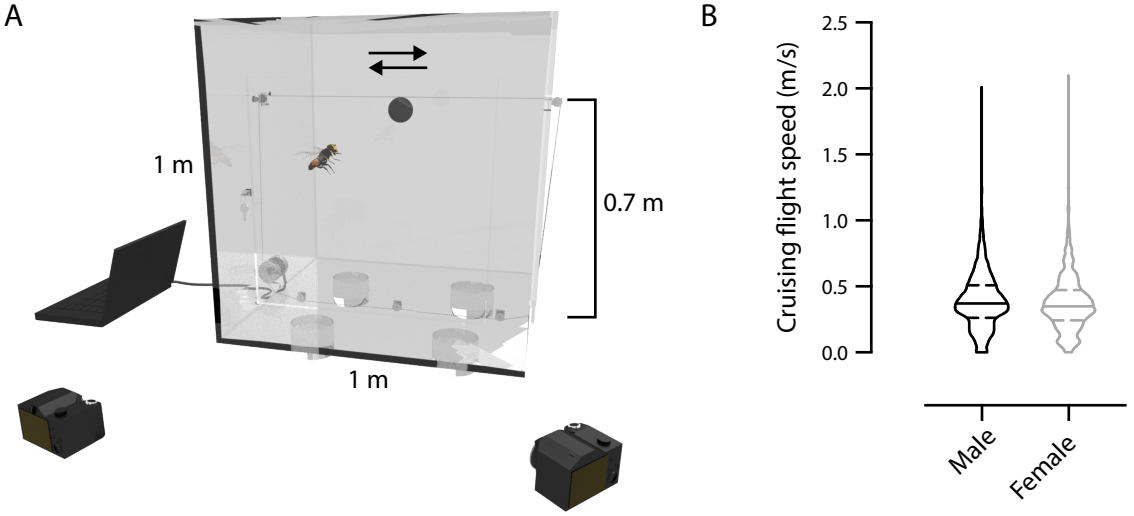
A
1 m
0.7 m
1 m
B
Cruising flight speed (m/s)
2.5
2.0
1.5
1.0
0.5
0.0
Male
Female

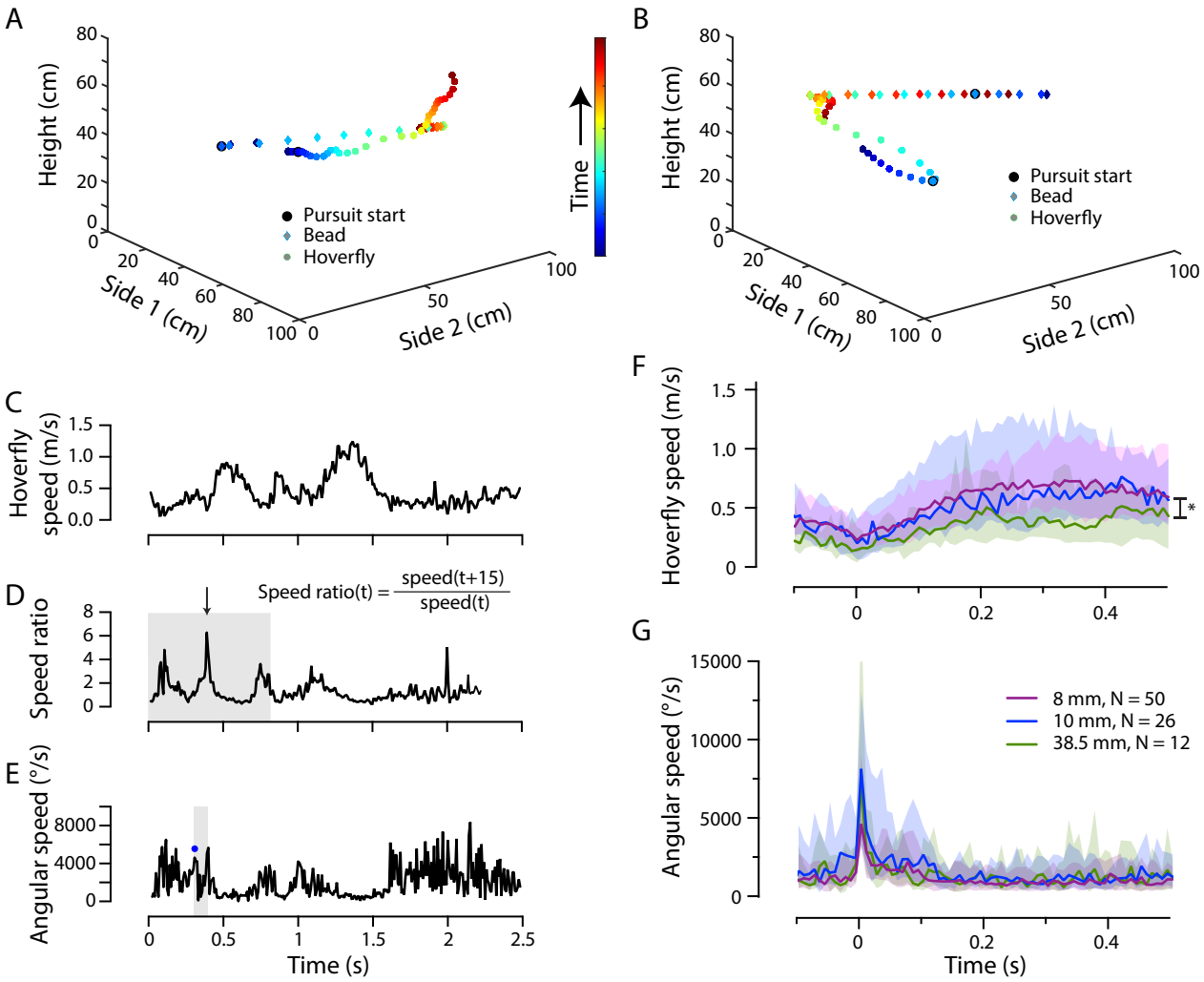
A
Height (cm)
Side 1 (cm)
Side 2 (cm)
Time
Pursuit start
Bead
Hoverfly
B
Height (cm)
Side 1 (cm)
Side 2 (cm)
Pursuit start
Bead
Hoverfly
C
Hoverfly speed (m/s)
D
Speed ratio
Speed ratio(t) = speed(t+15) / speed(t)
E
Angular speed (°/s)
Time (s)
F
Hoverfly speed (m/s)
G
Angular speed (°/s)
8 mm, N = 50
10 mm, N = 26
38.5 mm, N = 12
Time (s)

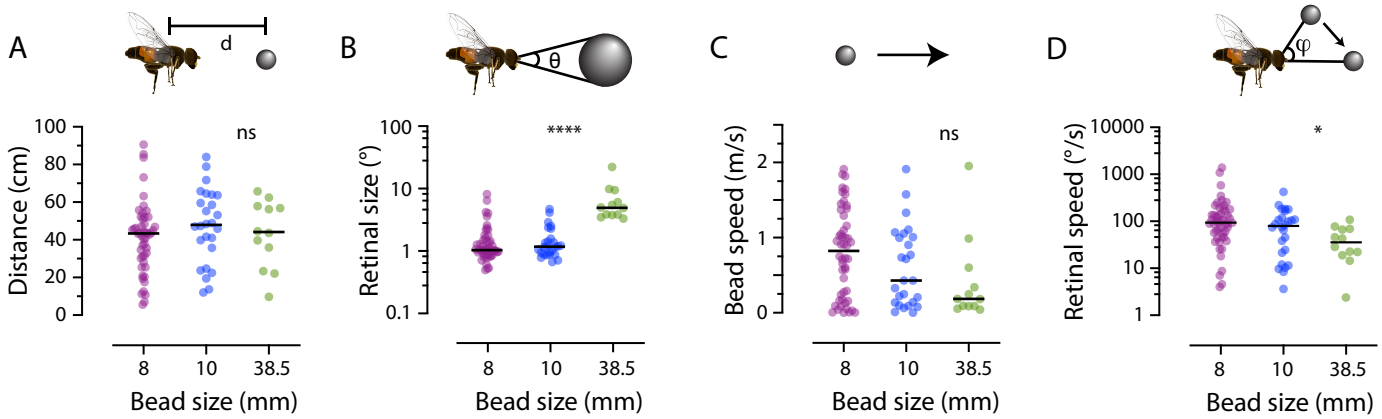
A
d
Distance (cm)
100
80
60
40
20
0
ns
8
10
38.5
Bead size (mm)
B
θ
Retinal size (°)
100
10
1
0.1
****
8
10
38.5
Bead size (mm)
C
Bead speed (m/s)
2
1
0
ns
8
10
38.5
Bead size (mm)
D
φ
Retinal speed (°/s)
10000
1000
100
10
1
*
8
10
38.5
Bead size (mm)

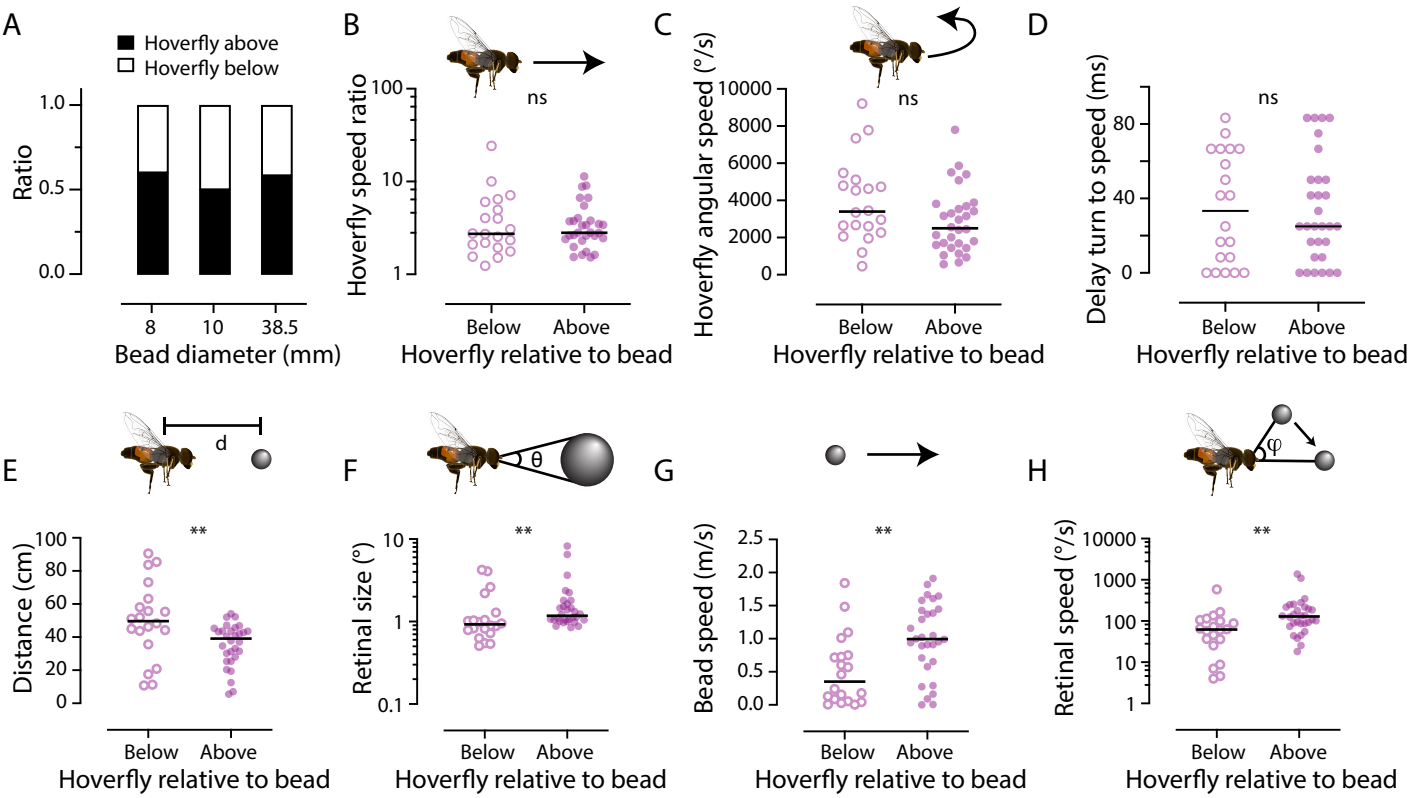
A
Hoverfly above
Hoverfly below
Ratio
1.0
0.5
0.0
8
10
38.5
Bead diameter (mm)
B
Hoverfly speed ratio
100
10
1
ns
Below
Above
Hoverfly relative to bead
C
Hoverfly angular speed (°/s)
10000
8000
6000
4000
2000
0
ns
Below
Above
Hoverfly relative to bead
D
Delay turn to speed (ms)
80
40
0
ns
Below
Above
Hoverfly relative to bead
E
d
Distance (cm)
100
80
60
40
20
0
**
Below
Above
Hoverfly relative to bead
F
θ
Retinal size (°)
10
1
0.1
**
Below
Above
Hoverfly relative to bead
G
Bead speed (m/s)
2.5
2.0
1.5
1.0
0.5
0.0
**
Below
Above
Hoverfly relative to bead
H
φ
Retinal speed (°/s)
10000
1000
100
10
1
**
Below
Above
Hoverfly relative to bead

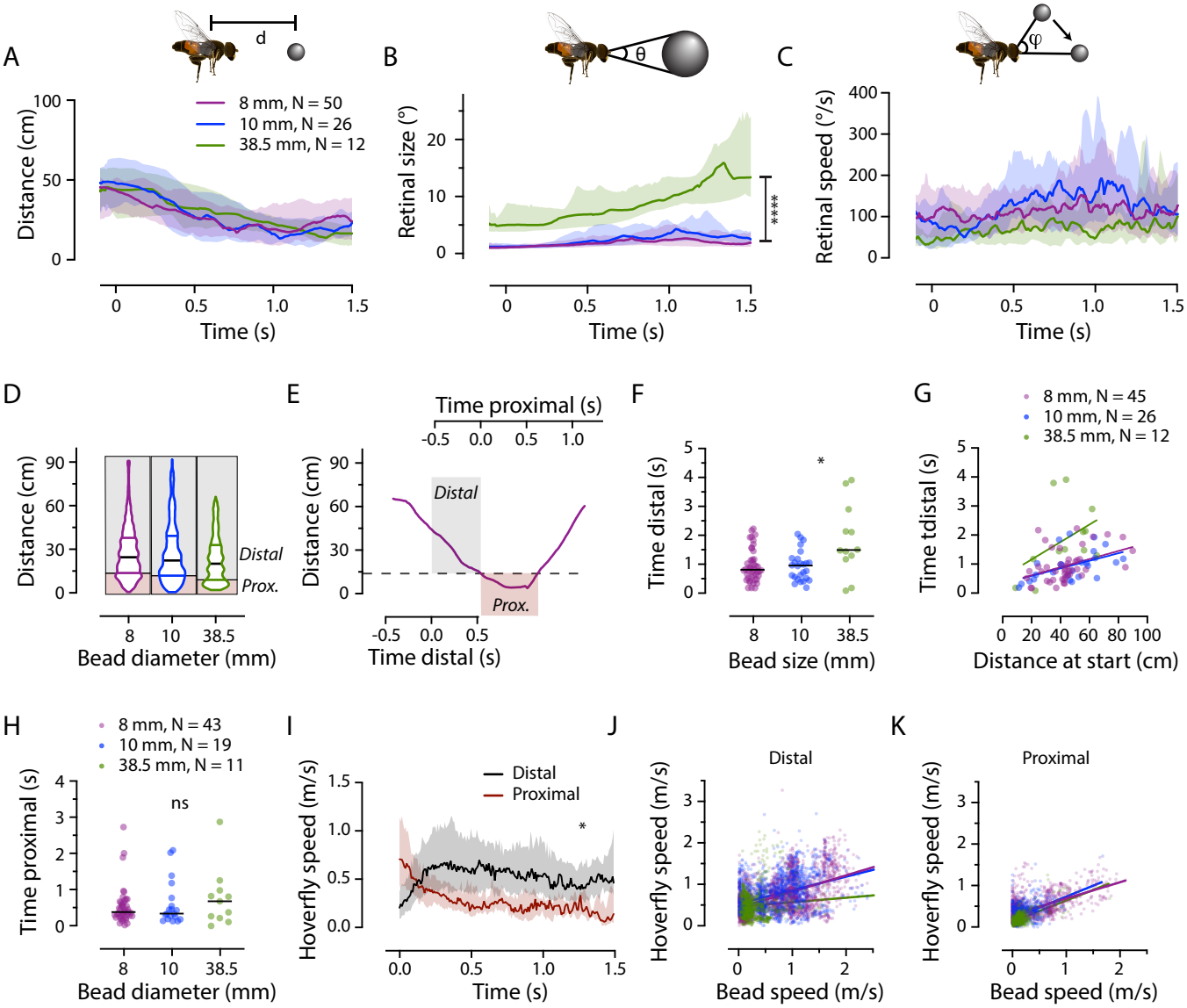
A
d
8 mm, N = 50
10 mm, N = 26
38.5 mm, N = 12
Distance (cm)
Time (s)
B
θ
Retinal size (°)
****
Time (s)
C
φ
Retinal speed (°/s)
Time (s)
D
Distance (cm)
Distal
Prox.
Bead diameter (mm)
E
Time proximal (s)
Distance (cm)
Distal
Prox.
Time distal (s)
F
Time distal (s)
*
Bead size (mm)
G
8 mm, N = 45
10 mm, N = 26
38.5 mm, N = 12
Time tdistal (s)
Distance at start (cm)
H
8 mm, N = 43
10 mm, N = 19
38.5 mm, N = 11
ns
Time proximal (s)
Bead diameter (mm)
I
Distal
Proximal
*
Hoverfly speed (m/s)
Time (s)
J
Distal
Hoverfly speed (m/s)
Bead speed (m/s)
K
Proximal
Hoverfly speed (m/s)
Bead speed (m/s)

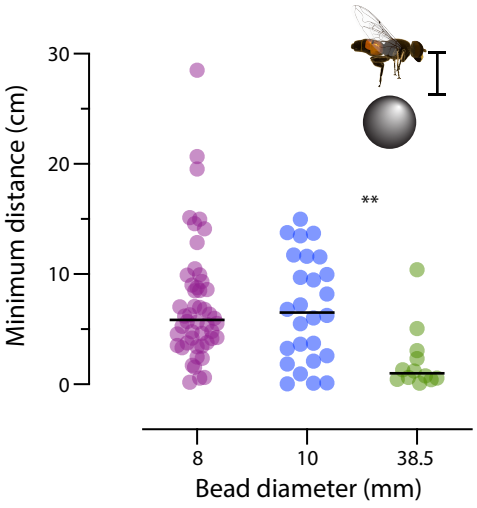
Minimum distance (cm)
30
20
10
0
**
8
10
38.5
Bead diameter (mm)

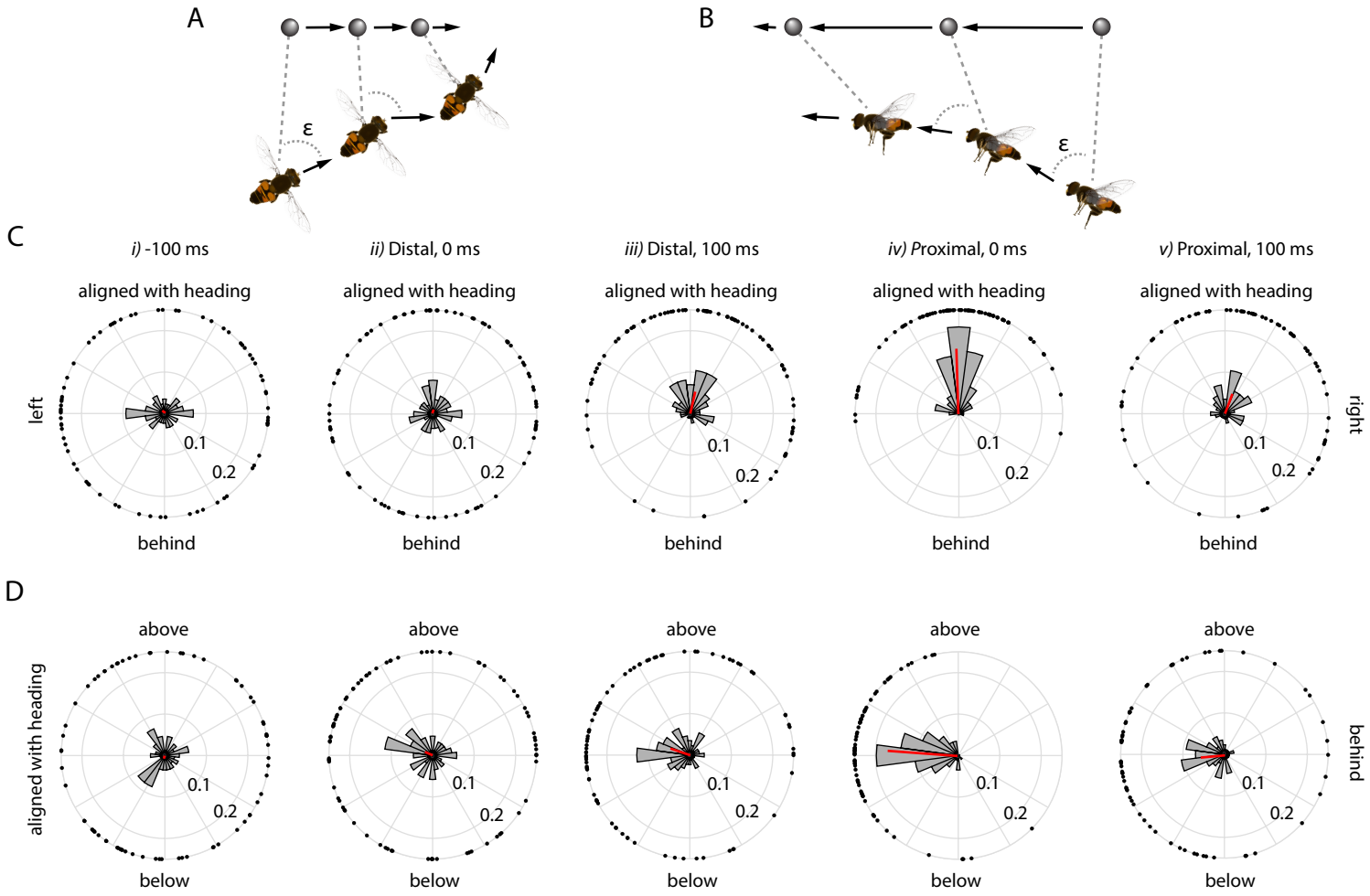
A
ε
B
ε
C
i) -100 ms
ii) Distal, 0 ms
iii) Distal, 100 ms
iv) Proximal, 0 ms
v) Proximal, 100 ms
aligned with heading
left
right
behind
0.1
0.2
D
above
below
aligned with heading
behind